Dual-Layer ℓ_1-Graph Embedding for Semi-supervised Image Labeling

Qian Wang[1(✉)], Guorong Wu[2], and Dinggang Shen[2]

[1] Med-X Research Institute, Shanghai Jiao Tong University, Shanghai, China
wang.qian@sjtu.edu.cn
[2] Department of Radiology and BRIC, University of North Carolina at Chapel Hill, Chapel Hill, USA

Abstract. In non-local patch-based (NLPB) labeling, a target voxel can fuse its label from the manual labels of the atlas voxels in accordance to the patch-based voxel similarities. Although state-of-the-art NLPB method mainly focuses on labeling a single target image by many atlases, we propose a novel semi-supervised strategy to address the realistic case of only a few atlases yet many unlabeled targets. Specifically, we create an ℓ_1-graph of voxels, such that each target voxel can fuse its label from not only atlas voxels but also other target voxels. Meanwhile, each atlas voxel can utilize the feedbacks from the graph to check whether its expert labeling needs to be corrected. The ℓ_1-graph is built by applying (dual-layer) sparsity learning to all target and atlas voxels represented by their surrounding patches. By embedding the voxel labels to the graph, the target voxels can jointly compute their labels. In the experiment, our method with the capabilities of (1) joint labeling and (2) atlas label correction has enhanced the accuracy of NLPB labeling significantly.

1 Introduction

Medical image labeling aims to parcellate each target image under consideration into individual anatomical structures, thus enabling region-based quantitative analyses within and across images. The technique has drawn intense attention from the community of medical image computing in recent years due to its importance to imaging-based clinical studies. Though manual labeling is still regarded as one of the most promising ways to generate the "ground truth", automatic methods are emerging as competitive solutions rapidly. In particular, automatic labeling has demonstrated its advantages of low cost and high efficiency in processing a huge number of images. The scales of related studies can thus become much larger, leading to more statistical powers of their findings.

Multi-atlas strategy has proven its effectiveness for automatic labeling of medical images. The strategy can be divided into three steps in general. *First*, a few atlases need to be manually delineated by human experts. *Then*, The expert labeling information is transferred to the unlabeled target images [1–3]. *Finally*, the contributions from the atlases are fused to label the target images [4–10]. In the simple *majority voting* (MV) method, for instance, all atlas and target

G. Wu et al. (Eds.): Patch-MI 2015, LNCS 9467, pp. 46–53, 2015.
DOI: 10.1007/978-3-319-28194-0_6

images are spatially normalized. Given each target voxel, the probability of its label can then be computed by counting the frequencies of the labels occurring at the same locations of all registered atlases.

A key notion for multi-atlas image labeling is that visually similar voxels in different images should have similar anatomical labels [6]. The *non-local patch-based* (NLPB) method [5] is a typical implementation bearing this notion. Specifically, all voxels can signify their visual appearances by their surrounding image patches for the computation of voxel similarity. Each target voxel may incorporate contributions from the non-local atlas voxels within a certain neighborhood. The contributions of the atlas voxels are adaptively fused regarding their visual similarities to the target voxel. The NLPB method, as well as its many variants, is widely applied to medical image labeling nowadays.

The NLPB method asks for as many atlases as possible, and handles the target images in a sequential order. However, this *many-to-one* scheme may not always function well in real clinical studies, as people tend to provide minimal yet high-cost expert labeling of the atlases. For example, researchers often manually label only a few healthy subjects as the atlases, and expect to further label other normal/pathological images automatically. In this scenario, we argue that a sophisticated *few-to-many* scheme can be better, since the introduction of more target images may contribute to labeling each other [1].

Motived by the above, we propose a novel *semi-supervised* strategy for the *few-to-many* NLPB labeling. Our method is capable of (1) jointly labeling all target images and (2) compensating for possible incorrect expert labeling of the atlases. Specifically, we create an ℓ_1-graph of voxels, such that each target voxel can fuse its label from the atlas voxels and other target voxels. At the same time, the atlas voxels can also utilize the feedbacks from the graph to check whether their expert labeling needs to be adjusted. The ℓ_1-graph is built by applying (dual-layer) sparsity learning to capture the similarities within all target and atlas voxels under consideration. By embedding the labels of all voxels to the ℓ_1-graph, the target voxels can compute their labels jointly.

2 Method

In NLPB labeling, each target voxel calculates the probability of its possible label based on the expert labeling transferred from the non-local atlas voxels. For convenience, we define a set of unlabeled target voxels (i.e., at the same locations of different target images) as $\mathcal{U}$ and a set of labeled atlas voxels (i.e., with potential contributions to $\mathcal{U}$) as $\mathcal{L}$ throughout this paper. Given $i \in \mathcal{U}$ and $j \in \mathcal{L}$, their appearances are signified by $\mathbf{x}_i$ and $\mathbf{x}_j$, respectively. In particular, $\mathbf{x}_i$ and $\mathbf{x}_j$ are often the vectorized image patches surrounding corresponding voxels (i.e., i and j). The length of $\mathbf{x}_i$ or $\mathbf{x}_j$ thus equals the size of the image patch. We further denote the probabilities of the labels of the voxels i and j as $\mathbf{y}_i$ and $\mathbf{y}_j$, respectively. The length of $\mathbf{y}_i$ or $\mathbf{y}_j$ is the same with the number of possible labels including the background. The task of NLPB labeling is then to estimate $\{\mathbf{y}_i, i \in \mathcal{U}\}$, given $\{\mathbf{x}_i, i \in \mathcal{U}\}$, $\{\mathbf{x}_j, j \in \mathcal{L}\}$, and $\{\tilde{\mathbf{y}}_j, j \in \mathcal{L}\}$.

Note that we deliberately use $\tilde{\mathbf{y}}_j$, instead of $\mathbf{y}_j$, to indicate that the labels of the atlas voxels are already known.

2.1 NLPB Labeling and Graph Embedding

Since similar voxels should have similar labels, we can compute the similarity between voxels based on their surrounding image patches and gauge the contributions from individual atlas voxels for determining the labels of the target voxels. Typically, we calculate the similarity between $\mathbf{x}_i$ and $\mathbf{x}_j$ following

$$w_{ij} = \exp\left(-\frac{\|\mathbf{x}_i - \mathbf{x}_j\|^2}{2\sigma^2}\right), \quad \forall i \in \mathcal{U}, \forall j \in \mathcal{N}_i \subseteq \mathcal{L}. \tag{1}$$

The label probability of the target voxel, namely $\mathbf{y}_i$, can then be fused by

$$\mathbf{y}_i = \frac{\sum_{j \in \mathcal{N}_i \subseteq \mathcal{L}} w_{ij} \tilde{\mathbf{y}}_j}{\sum_{j \in \mathcal{N}_i \subseteq \mathcal{L}} w_{ij}}, \quad \forall i \in \mathcal{U}. \tag{2}$$

The term $\mathcal{N}_i$ often qualifies the contributions from the non-local atlas voxels located within the neighborhood of each target voxel only. The NLPB model combining (1) and (2) can be reduced to MV by increasing σ to infinity and reducing the size of $\mathcal{N}_i$ to minimum. Meanwhile, we note that the labeling of individual target voxels are independent of each other as in the above.

We further interpret the NLPB labeling through the theory of graph embedding. For the target voxel $i \in \mathcal{U}$ specifically, it is contributed and connected by the atlas voxel $j \in \mathcal{N}_i$. The edge between them represents the contribution from j to i, and is assigned with the similarity measure w_{ij}. Then, the task of NLPB labeling is to embed the labels of all voxels in accordance to the graph that is derived from the similarities of image patches, following

$$\mathbf{y}_i = \arg\min_{\mathbf{y}_i} \sum_{j \in \mathcal{N}_i \subseteq \mathcal{L}} w_{ij} \|\mathbf{y}_i - \tilde{\mathbf{y}}_j\|^2, \quad \forall i \in \mathcal{U}. \tag{3}$$

It is easy to derive the solution that is exactly the same with (2). An illustration of the graph embedding process for NLPB labeling can be found in Fig. 1(a).

We aim to introduce the semi-supervised strategy for NLPB labeling. To this end, we re-write (3) to (4) as a summary of the proposed method, which is featured by:

1. All target voxels in $\mathcal{U}$ are jointly labeled. For a certain target voxel, the contributions to determine its label may come from not only the atlas voxels but also its connected target voxels in the graph (c.f. the first term in (4)).
2. The atlas voxels can deviate from their expert labeling adaptively (c.f. the second term in (4)), in order to alleviate the influences of possibly incorrect contributions from the atlases.

$$\{\mathbf{y}_i\}_{i \in \mathcal{U}} = \arg\min_{\{\mathbf{y}_i\}_{i \in \mathcal{U}}} \sum_{m \in \{\mathcal{U} \cup \mathcal{L}\}} \sum_{n \in \{\mathcal{U} \cup \mathcal{L}\}} w_{mn} \|\mathbf{y}_m - \mathbf{y}_n\|^2 + \alpha \sum_{j \in \mathcal{L}} \|\mathbf{y}_j - \tilde{\mathbf{y}}_j\|^2. \tag{4}$$

We will detail our solution to (4) in the form of graph embedding in the next.

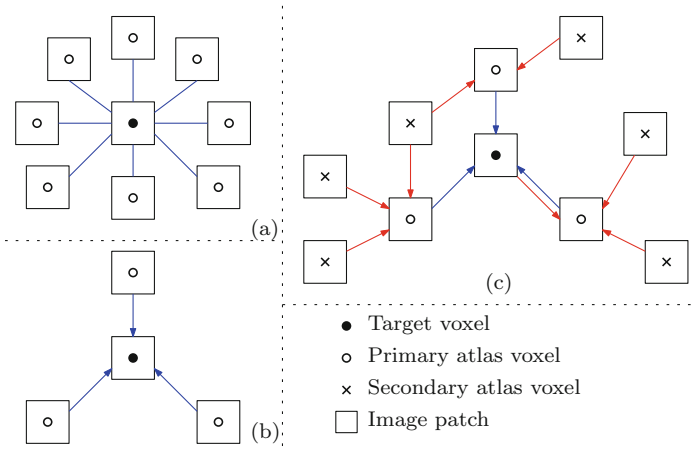

Fig. 1. NLPB labeling can be solved through graph embedding by: (a) the conventional method (e.g., [5]); (b) using the ℓ_1-graph; (c) the proposed method. Note that only a single target voxel is used for simplicity in this figure (Color figure online).

2.2 Laplacian-Based Embedding of ℓ_1-Graph

Graph Laplacian can help us solve (3) as well as (4). Specifically, we create an augmented matrix $\mathbf{Y} = \left[\mathbf{Y}^U, \tilde{\mathbf{Y}}^L\right]$, such that $\mathbf{y}_i$ $(i \in \mathcal{U})$ and $\tilde{\mathbf{y}}_j$ $(j \in \mathcal{L})$ are ordered as individual column vectors in $\mathbf{Y}^U$ and $\tilde{\mathbf{Y}}^L$, respectively. The adjacency matrix $\mathbf{W}$, which is filled in by w_{ij}, records the similarity between each pair of voxels. We then define the graph Laplacian of $\mathbf{W}$ as $\mathbf{\Delta} = \mathbf{D} - \mathbf{W}$. $\mathbf{D}$ is the diagonal degree matrix, where each diagonal entry is the sum of the corresponding row in $\mathbf{W}$. If the similarity is calculated by (1), both $\mathbf{W}$ and $\mathbf{\Delta}$ are symmetric. Thus, the problem in (3) is equivalent to minimize $\mathbf{Y}'\mathbf{\Delta}\mathbf{Y}$, as

$$\mathbf{Y}^U = -\tilde{\mathbf{Y}}^L \mathbf{\Delta}^{UL} \left(\mathbf{\Delta}^{UU}\right)^{-1}, \quad \mathbf{\Delta} = \begin{bmatrix} \mathbf{\Delta}^{UU} & \mathbf{\Delta}^{UL} \\ \mathbf{\Delta}^{LU} & \mathbf{\Delta}^{LL} \end{bmatrix}. \tag{5}$$

Our proposed method utilizes the ℓ_1-norm-based sparsity learning to estimate voxel similarity and thus build an ℓ_1-graph of voxels. An illustration of the ℓ_1-graph is available in Fig. 1(b). In the ℓ_1-graph, each target voxel only needs to consider the contributions from a limited number of most similar atlas/target voxels. By discarding many other redundant and confusing contributions, the labeling results can be more accurate [10]. Meanwhile, since the number of edges of the ℓ_1-graph is reduced due to sparsity constraint, the computation burden (i.e., regarding (5)) can be saved significantly.

In order to build the ℓ_1-graph, we first create a dictionary matrix $\mathbf{X} = \{\cdots, \mathbf{x}_m, \cdots\}$. Without loss of generality, the index m denotes all target and non-local atlas voxels under consideration. Then, the sparse representation of $\mathbf{x}_m$, regarding all other column vectors in $\mathbf{X}$, can be acquired through

$$\begin{aligned} \mathbf{w}_m &= \arg\min_{\mathbf{w}_m} \|\mathbf{x}_m - \mathbf{X}\mathbf{w}_m\|^2 + \beta\|\mathbf{w}_m\|_{\ell_1}, \\ \text{s.t.} \quad & w_{mn} \geq 0, w_{mm} = 0. \end{aligned} \tag{6}$$

The n-th entry in the coefficient vector $\mathbf{w}_m$, namely w_{mn}, is often perceived as the similarity from $\mathbf{x}_n$ to $\mathbf{x}_m$. Due to the ℓ_1-norm constraint controlled by β, there are only a few edges associated with each target voxel in the ℓ_1-graph.

It is worth noting that the embedding solution in (5) cannot be directly applied to the ℓ_1-graph. The reason is that the similarity measure derived from (6) is directional, leading to: (1) directed edges in the ℓ_1-graph (c.f. blue arrows in Fig. 1(b)); (2) asymmetry of $\mathbf{W}$ and $\mathbf{\Delta}$. To this end, we define a diagonal matrix $\mathbf{D}^*$, in addition to $\mathbf{D}$, as each diagonal entry in $\mathbf{D}^*$ is the sum of the corresponding column of $\mathbf{W}$. Then, $\mathbf{\Delta}^* = \mathbf{D}^* - \mathbf{W}'$ is defined to be the column graph Laplacian. It is shown by [11] that the optimization problem in (3) can be converted to minimize $\mathbf{Y}'\mathbf{C}\mathbf{Y}$, as the matrix $\mathbf{C} = \mathbf{\Delta} + \mathbf{\Delta}^*$ is symmetric. The labels of all target voxels can thus be jointly computed following

$$\mathbf{Y}^U = -\tilde{\mathbf{Y}}^L \mathbf{C}^{UL} \left(\mathbf{C}^{UU}\right)^{-1}, \quad \mathbf{C} = \begin{bmatrix} \mathbf{C}^{UU} & \mathbf{C}^{UL} \\ \mathbf{C}^{LU} & \mathbf{C}^{LL} \end{bmatrix}. \tag{7}$$

2.3 Dual-Layer Sparsity Learning

It is possible that certain atlas labeling is incorrect. Therefore, we allow the atlas voxels to deviate from their original labels in the proposed method (c.f. the second term in (4)). That is, the ℓ_1-graph not only transfers the labeling information from the atlases to the targets, but also provides feedbacks to individual atlases at the same time. Since the edges in the ℓ_1-graph are directed, we need to compute the inward edges for the atlas voxels. Specifically, we use the dual-layer sparsity learning approach as follows.

1. For each target voxel, we apply the first-layer sparsity learning (c.f. (6)). The target voxel is thus connected from the *primary* atlas voxels (i.e., in the set $\mathcal{P} \subseteq \mathcal{L}$) and other target voxels (i.e., in $\mathcal{U}$).
2. For each primary atlas voxel, the second-layer sparsity learning is applied. More *secondary* atlas voxels (i.e., in the set $\mathcal{S} \subseteq \mathcal{L} \backslash \mathcal{P}$) are incorporated into the graph. Note that the secondary atlas voxels are directly connected to the primary atlas voxels only, rather than the target voxels.

The dual-layer sparsity learning is illustrated by Fig. 1(c), where the edges of the first layer and the second layer are colored in blue and red, respectively. Other atlas voxels (in $\mathcal{L} \backslash \{\mathcal{P} \cup \mathcal{S}\}$) are inactive and thus excluded from the graph. In general, the ℓ_1-graph allows us to (1) compute the labels of the target voxels jointly and (2) adjust the expert labeling of the primary atlas voxels at the same time. Specifically, the objective function in (4) can be converted to minimize

$$\begin{bmatrix} \mathbf{Y}^U & \mathbf{Y}^P & \tilde{\mathbf{Y}}^S \end{bmatrix}' \begin{bmatrix} C^{UU} & C^{UP} & C^{US} \\ C^{PU} & C^{PP} & C^{PS} \\ C^{SU} & C^{SP} & C^{SS} \end{bmatrix} \begin{bmatrix} \mathbf{Y}^U & \mathbf{Y}^P & \tilde{\mathbf{Y}}^S \end{bmatrix} + \alpha \|\mathbf{Y}^P - \tilde{\mathbf{Y}}^P\|^2. \tag{8}$$

The closed-form solution to the above is

$$\begin{aligned}\mathbf{Y}^U = -\left(\alpha\tilde{\mathbf{Y}}^P - \tilde{\mathbf{Y}}^S\mathbf{C}^{SP}\right)\cdot\left(\mathbf{C}^{PP}+\alpha\mathbf{I}\right)^{-1}\cdot\mathbf{C}^{PU} \\ \cdot\left(\mathbf{C}^{UU}-\mathbf{C}^{UP}\left(\mathbf{C}^{PP}+\alpha\mathbf{I}\right)^{-1}\mathbf{C}^{PU}\right)^{-1}\end{aligned} \tag{9}$$

Note that (9) is equivalent to (5) and (7) when α is set to infinity. Therefore, our method can be regarded as a generalized form of the NLPB labeling.

2.4 Summary

We briefly summarize the proposed method as follows:

1. For a certain location, we extract all image patches regarding $\mathcal{U}$ and $\mathcal{L}$;
2. We apply sparsity learning to $\mathcal{U}$ and acquire the first layer of the ℓ_1-graph;
3. Sparsity learning is further applied to reveal the second layer of the graph;
4. The labels of all target voxels are jointly embedded following (9).

3 Experimental Results

In order to demonstrate the capability of the proposed method, we apply it to hippocampus labeling of brain MR images. In particular, we randomly select 10 atlas and 60 target images from the Alzheimer's Disease Neuroimaging Initiative (ADNI) database. All atlas images are from healthy subjects. The target images can be divided into three equally-sized sub-groups, corresponding to the subjects of health control (HC), mild cognitive impairment (MCI), and the Alzhermer's disease (AD), respectively. It is worth noting that MCI is typically regarded as a transitional stage between HC and AD. Meanwhile, abnormal atrophy of the hippocampus is closely related to AD, making the morphology of the hippocampus an important bio-marker to AD diagnosis and treatment [12].

After standard pre-processing (i.e., bias correction, skull-stripping, histogram matching, and affine registration), we utilize the 10 HC atlases to label the 60 targets by the proposed method (designated as "Proposed III" in Table 1) and four alternatives. In addition to the well-known "MV" and "NLPB" [5] methods, "Sparse-NLPB" computes the similarities between the target and the non-local atlas voxels via sparsity learning. "Joint-NLPB" [10], a latest NLPB variant, allows each atlas voxel to estimate the confidence of its contribution by interacting with other atlas voxels through a generative probability model. Note that all four existing methods label individual target voxels sequentially, in contrary to the joint labeling style in our method.

We evaluate the Dice ratio, a widely accepted metric, as the indicator of the labeling quality. The Dice ratio measures the overlapping between the multi-atlas labeling result and the expert labeling in the ADNI database, as higher Dice ratio often implies more accurate labeling. The Dice ratios of individual methods are compared in Table 1. The scores are averaged over the left/right hippocampus across target images already. For fair comparison, all voxels are

signified by $5\times5\times5$ image patches. The size of the non-local search neighborhood is $9 \times 9 \times 9$. We set β to 0.1 for the fist-layer sparsity learning of our method and for Sparse/Joint-NLPB as recommended by [10]. In the second layer of our method, however, we increase β to 0.2 for selecting fewer secondary atlas voxels and also less computation. The parameter α is arbitrarily set to 5.

Table 1. The Dice ratios of hippocampus labeling through different methods.

Method	HC	MCI	AD	Overall
MV	0.591 ± 0.078	0.589 ± 0.089	0.566 ± 0.111	0.582 ± 0.093
NLPB	0.682 ± 0.042	0.675 ± 0.040	0.660 ± 0.061	0.672 ± 0.048
Sparse-NLPB	0.729 ± 0.035	0.704 ± 0.039	0.684 ± 0.048	0.706 ± 0.041
Joint-NLPB	0.755 ± 0.027	0.733 ± 0.038	0.719 ± 0.046	0.736 ± 0.037
Proposed I	0.742 ± 0.027	0.720 ± 0.044	0.691 ± 0.050	0.718 ± 0.040
Proposed II	0.741 ± 0.028	0.728 ± 0.041	0.716 ± 0.045	0.728 ± 0.038
Proposed III	$\mathbf{0.756 \pm 0.025}$	$\mathbf{0.750 \pm 0.040}$	$\mathbf{0.744 \pm 0.041}$	$\mathbf{0.750 \pm 0.035}$

As in Tabel 1, our method (Proposed III) yields significantly higher Dice ratio in overall, compared to the four existing methods. We note that the performances of our method and Joint-NLPB are close for the target images of HC. However, regarding MCI and AD where hippocampus labeling is more difficult in general, our method owns a large margin ahead. We attribute this improvement to the introduction of the semi-supervised strategy, which enables (1) joint labeling of all target voxels and (2) adaptive label correction for primary atlas voxels.

We design two degraded cases of our method for further evaluation. In "Proposed I", each HC/MCI/AD sub-group of 20 target images is jointly labeled. In "Proposed II", all three sub-groups of 60 target images are jointly labeled. The parameter β is set to infinity for both Proposed I and II, such that the primary atlas voxels follow their expert labeling strictly. Comparing Proposed I to (Sparse-)NLPB, the joint labeling strategy has shown its advantages in all three sub-groups. Comparing Proposed II to I, we conclude that the introduction of more target images leads to better labeling quality, especially for the MCI/AD target images whose appearances are less similar to the atlases. Comparing Proposed III to II, we conclude that the primary atlas voxels can effectively correct their original labels and thus improve their contributions to the target voxels, once the secondary atlas voxels are incorporated.

4 Discussion

We have proposed a semi-supervised patch-based labeling method, and applied it to hippocampus labeling for brain MR images. Specially, we build a dual-layer ℓ_1-graph of voxles, and jointly label all target voxels through graph embedding.

The dual-layer graph topology is "deeper" than the flat design of most state-of-the-art methods, where atlas voxels are directly connected to the target voxels only. In our method, however, the primary atlas voxels can interact with the graph to adjust its original expert labeling. In this way, the contributions of the atlas voxels can become much more accurate.

Our method well fits the clinical studies in which a few atlas images are expected to label many targets. To this end, we have shown that it is necessary to incorporate all target images for the joint labeling. It is also worth noting that the accuracy of multi-atlas labeling is strongly dependent on the number and the composition of the atlases. To this end, we will investigate a possible way to select the minimal number of optimal atlases in future. We will also work on to improve the speed performance of our method.

References

1. Wolz, R., Aljabar, P., Hajnal, J.V., Hammers, A., Rueckert, D., Initiative, A.D.N., et al.: Leap: learning embeddings for atlas propagation. NeuroImage **49**(2), 1316–1325 (2010)
2. Jia, H., Yap, P.T., Shen, D.: Iterative multi-atlas-based multi-image segmentation with tree-based registration. Neuroimage **59**(1), 422–430 (2012)
3. Zikic, D., Glocker, B., Criminisi, A.: Encoding atlases by randomized classification forests for efficient multi-atlas label propagation. Med. Image Anal. **18**(8), 1262–1273 (2014)
4. Sabuncu, M.R., Yeo, B.T., Van Leemput, K., Fischl, B., Golland, P.: A generative model for image segmentation based on label fusion. IEEE Trans. Med. Imaging **29**(10), 1714–1729 (2010)
5. Coupé, P., Manjón, J.V., Fonov, V., Pruessner, J., Robles, M., Collins, D.L.: Patch-based segmentation using expert priors: application to hippocampus and ventricle segmentation. NeuroImage **54**(2), 940–954 (2011)
6. Rousseau, F., Habas, P.A., Studholme, C.: A supervised patch-based approach for human brain labeling. IEEE Trans. Med. Imaging **30**(10), 1852–1862 (2011)
7. Asman, A.J., Landman, B.A.: Non-local STAPLE: an intensity-driven multi-atlas rater model. In: Ayache, N., Delingette, H., Golland, P., Mori, K. (eds.) MICCAI 2012, Part III. LNCS, vol. 7512, pp. 426–434. Springer, Heidelberg (2012)
8. Wachinger, C., Golland, P.: Spectral label fusion. In: Ayache, N., Delingette, H., Golland, P., Mori, K. (eds.) MICCAI 2012, Part III. LNCS, vol. 7512, pp. 410–417. Springer, Heidelberg (2012)
9. Wang, H., Suh, J.W., Das, S.R., Pluta, J.B., Craige, C., Yushkevich, P.A.: Multi-atlas segmentation with joint label fusion. IEEE Trans. Pattern Anal. Mach. Intell. **35**(3), 611–623 (2013)
10. Wu, G., Wang, Q., Zhang, D., Nie, F., Huang, H., Shen, D.: A generative probability model of joint label fusion for multi-atlas based brain segmentation. Med. Image Anal. **18**(6), 881–890 (2014)
11. Yan, S., Wang, H.: Semi-supervised learning by sparse representation. In: SDM, pp. 792–801. SIAM (2009)
12. Thompson, P.M., Hayashi, K.M., de Zubicaray, G.I., Janke, A.L., Rose, S.E., Semple, J., Hong, M.S., Herman, D.H., Gravano, D., Doddrell, D.M., et al.: Mapping hippocampal and ventricular change in alzheimer disease. Neuroimage **22**(4), 1754–1766 (2004)